Computer-Aided Detection Methods Using Hyperspectral Imaging Engineering

Subjects: Oncology
Contributor: Hung-Yi Huang , Yu-Ping Hsiao , Riya Karmakar , Arvind Mukundan , Pramod Chaudhary , Shang-Chin Hsieh , Hsiang-Chen Wang

Skin cancer, a malignant neoplasm originating from skin cell types including keratinocytes, melanocytes, and sweat glands, comprises three primary forms: basal cell carcinoma (BCC), squamous cell carcinoma (SCC), and malignant melanoma (MM). BCC and SCC, while constituting the most prevalent categories of skin cancer, are generally considered less aggressive compared to MM. Notably, MM possesses a greater capacity for invasiveness, enabling infiltration into adjacent tissues and dissemination via both the circulatory and lymphatic systems. Risk factors associated with skin cancer encompass ultraviolet (UV) radiation exposure, fair skin complexion, a history of sunburn incidents, genetic predisposition, immunosuppressive conditions, and exposure to environmental carcinogens. Early detection of skin cancer is of paramount importance to optimize treatment outcomes and preclude the progression of disease, either locally or to distant sites. In pursuit of this objective, numerous computer-aided diagnosis (CAD) systems have been developed. Hyperspectral imaging (HSI), distinguished by its capacity to capture information spanning the electromagnetic spectrum, surpasses conventional RGB imaging, which relies solely on three color channels.

skin cancer hyperspectral imaging melanoma

1. Introduction

Skin cancer is mainly encountered in people with a lighter skin complexion [1]. It can most often be found in countries like the United States of America, Germany, China, and France [2]. Skin cancer currently represents one-third of all cancer diagnoses worldwide, and the number of cases has been continuously increasing in recent years [3]. Skin cancer can be classified as non-melanoma skin cancer (NMSC) or melanoma [4]. In 2018, non-small cell lung cancer (NMSC) was the fifth most common form of cancer worldwide (excluding basal-cell carcinomas, or BCCs), accounting for over one million different detections and approximately sixty-five thousand deaths, while malignancy was the current century's most common form of cancer, accounting for nearly 300,000 new cases and 60,000 deaths [5][6][7][8][9]. The prevalence of the two types of non-melanoma and melanoma cancers of the skin has exhibited an upward trend in recent decades [10][11][12]. Presently, the annual incidence of non-melanoma skin cancers (NMSC) ranges from 2 to 3 million cases worldwide, whereas the occurrence of melanoma skin cancers amounts to approximately 132,000 cases globally. [13]. The estimated number of new cases of skin cancers (excluding BCC and SCC) in the US in 2022 is 108,480, with 62,820 in males and 45,660 in females [14][15][16][17]. The total number of melanoma skin cancers is 99,780, with 57,180 in males and 42,600 in females [18]. There are

8700 cases of other non-epithelial skin cancer, with 5640 in males and 3060 in females [19]. Among these, the estimated deaths of skin cancers in the US in 2022 were 11,990, with 8060 males and 3930 females [20][21][22]. In melanoma skin cancer, the estimated death cases are 7650: 5080 in males and 2570 in females [23]. Out of the 8700 other non-epithelial skin cases, the estimated number of mortality cases is 4340: 2980 for males and 1360 for females [24]. In a study, the analysis examines the ten-year rate of survival for melanoma individuals in Japan between 1987 and 2001 [25]. The data indicates that the survival rate among female patients was comparatively greater than that among male patients. Specifically, the 140-month survival rate was found to be 70.6% for females, while it stood at 60% for males [26]. Carcinoma was the leading cause of mortality among individuals diagnosed with skin cancer and blackfoot disease [27]. After the commencement of blackfoot illness, the five-year survival rate was 76.3%, the 10-year survival rate was 63.3%, and the 15-year survival rate was 52.2% [28]. Sixteen years after the first symptoms of the illness appeared, the survival rate dropped to 50 percent [29][30][31].

Computer-aided diagnosis (CAD) is good for cancer detection because it uses artificial intelligence, machine learning models, algorithms, and data acquisition from automated or computerized tools [32][33][34][35]. Zhiying et al. conducted a study in which they used an advanced method of image segmentation that was based on the convolutional neural network (CNN) specifically developed by satin bowerbird optimization (SBO). The study's primary objective was to reduce image noise in order to achieve higher levels of productivity, as shown by the confusion matrix [36]. In another study by Jaleel et al., imaging techniques and artificial intelligence using artificial neural network (ANN) machine learning technology were used for skin diagnosis instead of going to the hospital [37][38][39]. Biosensors are devices that are designed to detect a specific biological analyte by essentially converting a biological entity into an electrical signal that can be detected and analyzed [40][41][42]. The technology of biosensors has the ability to enable rapid and precise detection, dependable imaging of cancerous cells, and management of cancer spread and angiogenesis [43]. Research conducted by Keshvarz et al. uses water-based tetrahertz metamaterial as a biosensor for the early detection of skin by analyzing image features and characteristics [44]. In another study, Bohunickey et al. used Indium Gallium Arsenide (InGaAs) as a biosensor to analyze pigmented skin lesions within specified wavelength ranges from 414 nm to 995 nm [45]. Nowadays, CAD and biosensors are usually not utilized for skin cancer diagnosis because the biosensor parameter will change according to pressure [46][47][48] and temperature, and it will sometimes give wrong information about images, which is unsuitable for the early detection of cancer [49]. CAD models are also not effective when the user commands the wrong input during data acquisition, and they will not work effectively [50][51][52][53][54].

One of the non-invasive optical imaging systems that can overcome all the aforementioned challenges and complications is HSI [55]. HSI is capable of combining digital imagery with techniques of spectroscopy, which provides enhanced spectral qualities of a recorded picture both within the visible range of the electromagnetic spectrum as well as beyond it [56][57]. In a hyperspectral image, each pixel at each wavelength is analyzed, resulting in a so-called spectral signature [58]. The spectral signature stores all of the spatial data that correspond to a certain substance or picture and its location in space [59]. It has been shown that quantifiable data on tissue biology may be obtained via spectral signature analysis [60]. The HSI technique can overcome the drawbacks of CAD and biosensors as it will analyze each spectral wavelength and data from the signature spectrum with deep penetration of the materials [61][62]. Hyperspectral imaging (HSI) techniques are applied in various fields, including

aerospace [63], food technology [64], agriculture [65], medical field [66][67], astronomy [68], skin cancer [69][70][71], breast cancer [72], remote sensing [73], satellite imaging [74], seed viability study [75], biotechnology [76], biosensor [77], environmental monitoring [78][79], counterfeit detection [80][81][82][83], pharmaceuticals [84], medical diagnose [85][86], forensic science [87], thin films [88], oil and gas [89], microbiology [90], chemical industry [91], esophagus cancer [92], spectrum analysis [93], brain tumor [94], nursing [95], physical therapy [96], and surgery [97].

2. Methods of Skin Cancer Detection

There are various traditional methods of skin cancer detection, and early identification is the key to better and more effective treatment of the skin lesions [98]. The knowledge of dermatologists and the results of pathological examinations of biopsy specimens are often relied upon to diagnose skin cancer [99]. The standard imaging methods, such as multispectral imaging (MSI), are used in the morphological processing algorithms that underpin the diagnostic assistance system [100]. In the industry of dermatology, one of the basic guidelines for pigmented skin lesion diagnosis is the ABCD rule [101]. Many characteristics of skin lesions are represented by their corresponding letters in the ABCD rule, and these characteristics include asymmetry of the mole, border irregularity, color uniformity, diameter, and evolving size, shape, or color rule [102]. After this observation, a biopsy is prepared when a dermatologist suspects that the skin lesions are infected [103]. After that, a pathological examination of the material is carried out so that a definite diagnosis may be determined [104][105][106]. A number of methods, depending on image data and techniques, integrate the ABCD principle to aid doctors in their regular diagnostic practice for evaluating and classifying pigmented skin lesions (PSL) [107][108][109]. When applying the ABCD rule to diagnose a skin lesion, a score is assigned for each of the four features of the ABCD rule and combined into a total score [110][111]. The total score determines the level of malignancy of the sample taken, where a higher score means a greater level of malignancy [112]. In clinical experiments, the reported sensitivity and specificity of the ABCD rule are in the ranges of 74–91.6% and 45–67%, respectively [113]. Different types of skin cancer, including BCC, SCC, SK, and non-epithelial skin cancer, are shown in **Figure 1** [114].

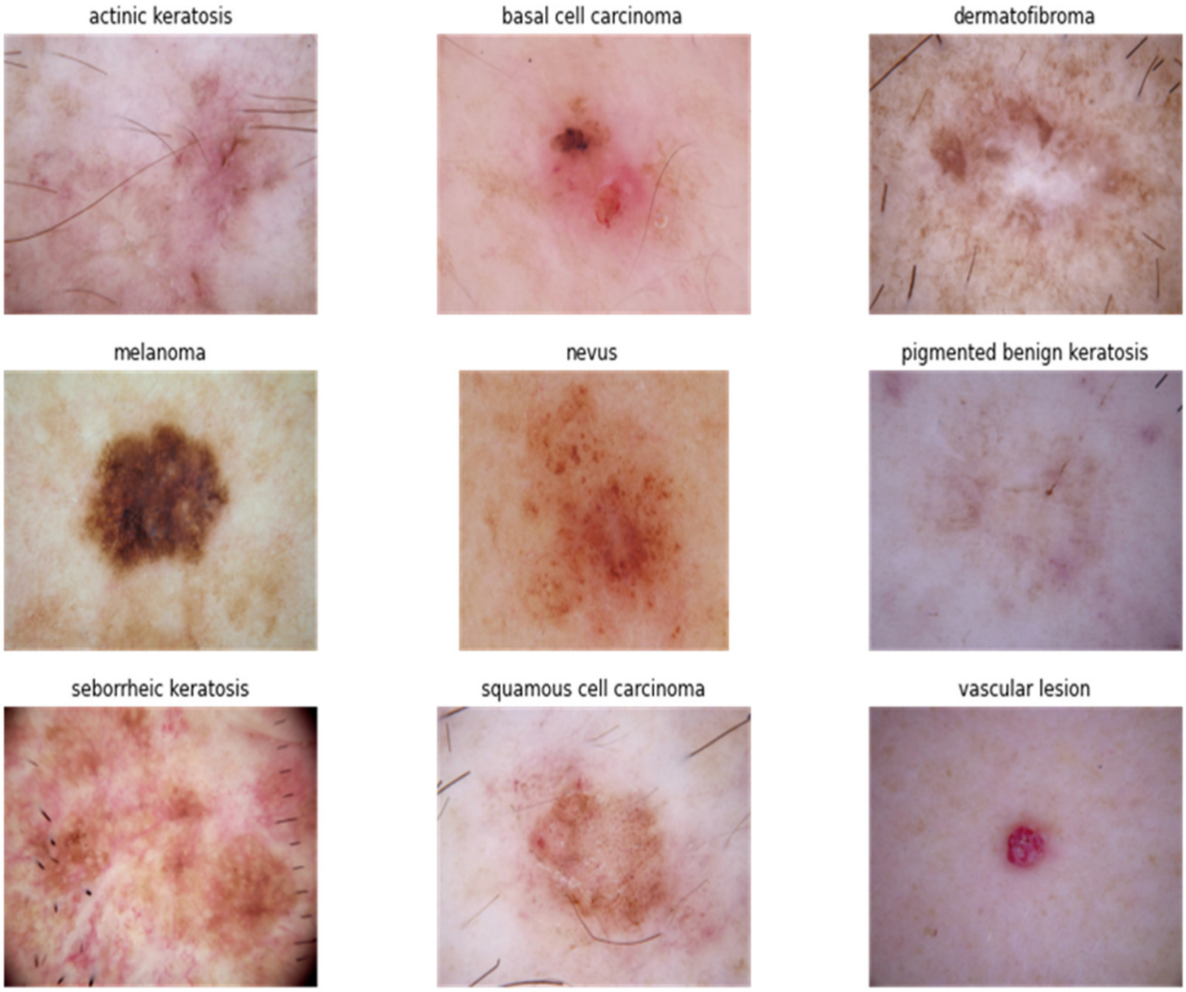

Figure 1. Types of skin cancers retrieved from the ISIC dataset.

Due to the fact that traditional technology does not place an emphasis on spatial and spectral information, a normal eye or smart phone is unable to identify melanoma and BCC in the early stages of skin cancer [115][116][117][118]. Over the course of the last several years, scientists from a wide variety of disciplines have collaborated on the expansion and development of novel dermoscopic technologies for the early diagnosis of skin cancer, as well as the formulation of diagnostic criteria and computer algorithms [119][120][121]. For example, the ABCD rule has been extended to ABCDE, where the E represents the evolution of the skin lesion over time [122]. With the advancement of machine learning and computerized algorithms, several research groups have been concentrating on developing automated and semi-automated computational methods for detecting and classifying skin lesions [123][124][125]. In addition, researchers focused on conventional RGB (red, green, blue) imaging techniques and dermoscopic imaging techniques and found out the difference between conventional and dermoscopic imaging techniques. Conventional imaging deals with visual inspection, observation, and changes in shape, size, and color, whereas dermoscopy imaging techniques deal with computerized algorithms and tools and easily differentiate skin melanoma [99][126][127].

3. Computer-Aided Detection Methods Using Hyperspectral Imaging Engineering to Detect Skin Cancer

The graphical representation of the quantitative findings pertaining to skin cancer detection, derived from a meta-analysis of skin cancer studies, was achieved by the use of the forest plot and Deek's funnel plot. The forest plots were used to analyze the sensitivity and specificity of each CAD approach, taking into account factors such as nationality, kind of skin cancer, band area, year of publication, and the individual studies as shown in **Figure 2**. These analyses were conducted at a 95% confidence level [128]. A forest plot is a visual depiction of the findings derived from a meta-analysis, as shown by scholarly sources [129][130][131]. This research presents the outcomes of research conducted using a 95% confidence interval, including both positive and negative error values [132]. A wider range of confidence intervals is associated with less precise findings, whereas a narrower range of confidence intervals indicates more precision in the obtained results [133]. The dashed line seen in the forest plot symbolizes the threshold for inaction. In the context of the specificity forest plot, the studies conducted by Zherdeva et al. and Pozhar et al. align with the line of no action, indicating that these particular studies have less significance for the pooled meta-analysis. This implies that the *p*-values of the aforementioned studies exceed a confidence interval of 0.005. Specifically, the investigations conducted by Leon et al., Lindholm et al., Pardo et al., Vinokuro et al., Rasanen et al., and T. Nagaoka et al. fall on the positive side of the line of no action, indicating that these studies were statistically significant for the purpose of the meta-analysis. The investigations conducted by Christens et al. and Hosking et al. are positioned on the left side of the line of no action, indicating that these studies do not provide statistically significant results for inclusion in a pooled meta-analysis. The diamond shape is used to represent the magnitude of separate research weights, as well as the precision of their respective findings, as shown by the range of the confidence interval. In the context of the meta-analysis, it can be seen that the studies conducted by Christens et al. and Pardo et al. exhibit lower levels of significance. Conversely, the studies conducted by Hosking et al., Rasanen et al., and T. Nagaoka et al. have higher levels of significance. The investigations conducted by Lindholm et al., Pozhar et al., Vinokuro et al., and Zherdeva et al. are not considered substantial for inclusion in a pooled meta-analysis.

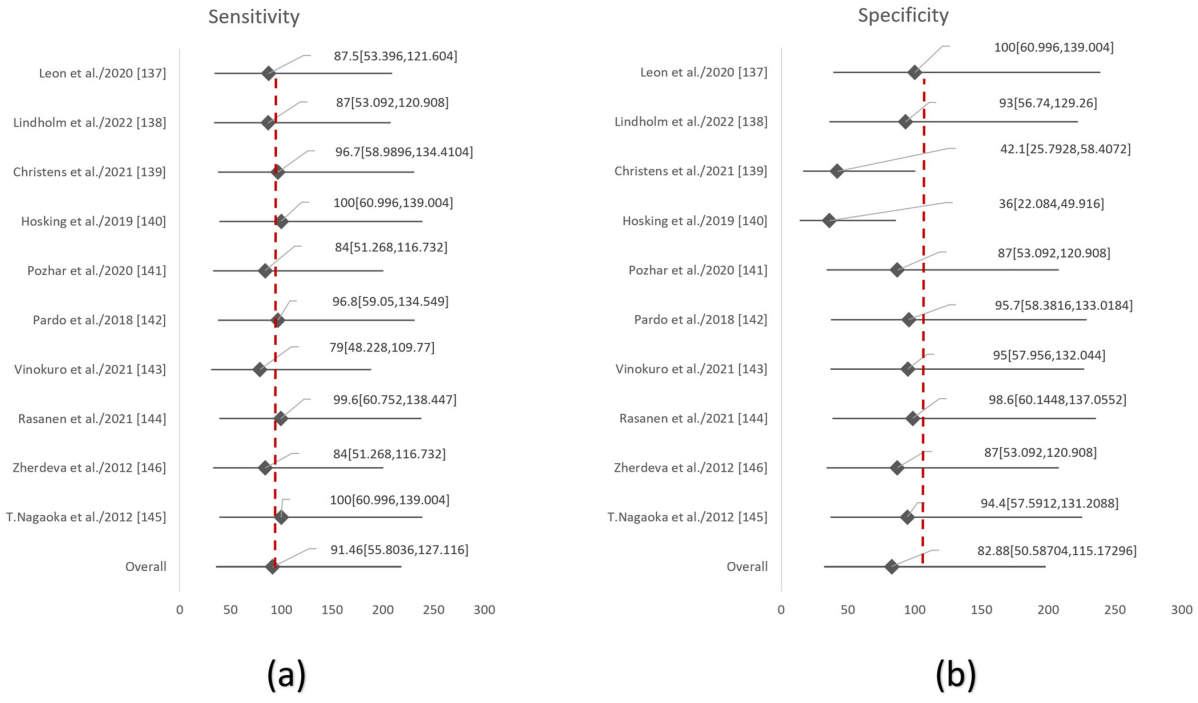

Figure 2. Forest plots based on the (**a**) sensitivities and (**b**) specificities of overall studies.

The research concluded by presenting Deek's funnel plots, which were categorized based on many factors, including the CAD technique, country, skin cancer kind, year of publication, and band region as shown in **Figure 3**. These plots were constructed with a confidence level of 95% for each study included in the analysis. The funnel plot developed by Deek incorporates the odds diagnostic ratio on the *x*-axis and the proportion of the square root of each sample size on the *y*-axis [134][135][136]. The funnel plots developed by Deek provide a comprehensive representation of the regression line and confidence values for each study, facilitating a comparative analysis between the *x* and *y* axes [137]. Deek's funnel plot is a graphical representation of the relationship between the mean effect size and the standard error (SE). This figure presents a comparison of the degree of variance seen across several studies [138]. The funnel plot displays symmetrical findings, indicating an equal distribution of studies above and below the mean regression line, which represents the standard error versus the odds ratio. The analysis of the funnel plot suggests that both the SKL and CNN exhibit significant standard error values but very low odds ratios. SVM and DI models exhibit high standard error values and odd ratios that are somewhat less diverse, as shown by a *p*-value of 0.813591, which is above the threshold of 0.005. Consequently, these findings suggest a higher level of heterogeneity, with a standard error of 4.39553. In comparison, Western research has higher standard error values and odds ratios when compared to Asian studies, with a regression line of 1.025.

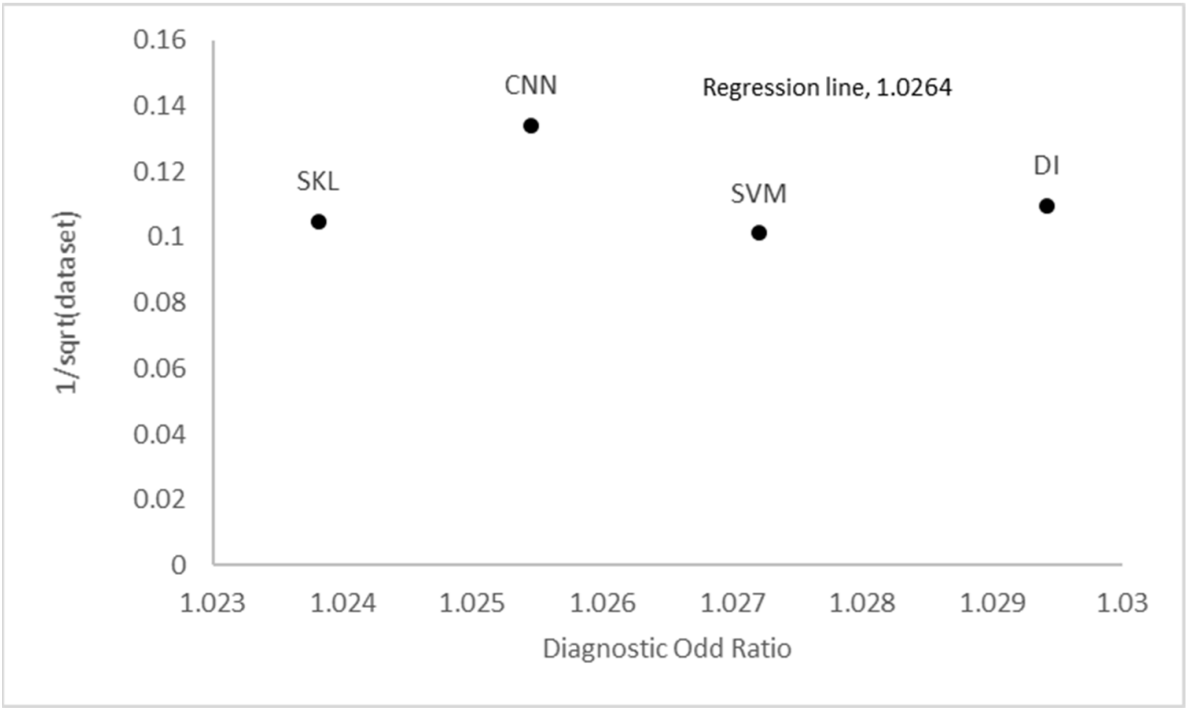

Figure 3. Deek's funnel plot based on CAD methods.

While the systematic literature review and meta-analysis have provided valuable insights into the current landscape of skin cancer detection using HSI, several avenues for future research emerge. First, efforts should be directed toward standardizing data collection protocols and imaging technologies, as the heterogeneity in studies can impact the comparability of results. Second, exploring the integration of AI and machine learning algorithms with

HSI for real-time and automated skin cancer detection holds significant promise. Third, enhancing the portability and affordability of HSI devices can expand their accessibility in clinical settings. Additionally, the development of user-friendly software tools for HSI data analysis and interpretation is essential. Further studies could also investigate the use of HSI in diverse skin types and ethnic populations to assess its robustness across demographics. Lastly, collaborative, interdisciplinary research involving clinicians, engineers, and data scientists is crucial for advancing the field and translating HSI-based skin cancer detection into routine clinical practice. The proposed approach in this research is not without its limitations, which are essential to acknowledge for a comprehensive understanding of the research. While the systematic literature review and meta-analysis have provided valuable insights, it is important to note that the quality and heterogeneity of the included studies can influence the generalizability of the findings. The variability in data collection protocols, imaging technologies, and sample sizes across the selected studies may introduce some degree of bias and limit the direct comparability of results. Additionally, the evolving nature of HSI technology and the relatively limited number of studies available for analysis may have implications for the current state of the field. Furthermore, the majority of the studies reviewed predominantly focused on specific skin cancer types or populations, potentially affecting the applicability of the conclusions to broader contexts. Lastly, while promising trends and potential areas of improvement have been identified, the translation of HSI-based skin cancer detection into clinical practice may encounter practical challenges, such as cost-effectiveness and regulatory considerations. This scarcity of eligible studies highlights the nascent stage of HSI research in this specific application. Acknowledging these limitations is crucial for a nuanced interpretation of the findings and underscores the need for further research to address these challenges and refine the use of HSI in clinical applications.

References

1. Gupta, A.K.; Bharadwaj, M.; Mehrotra, R. Skin cancer concerns in people of color: Risk factors and prevention. Asian Pac. J. Cancer Prev. APJCP 2016, 17, 5257.
2. Sung, H.; Ferlay, J.; Siegel, R.L.; Laversanne, M.; Soerjomataram, I.; Jemal, A.; Bray, F. Global cancer statistics 2020: GLOBOCAN estimates of incidence and mortality worldwide for 36 cancers in 185 countries. CA A Cancer J. Clin. 2021, 71, 209–249.
3. Leiter, U.; Keim, U.; Garbe, C. Epidemiology of skin cancer: Update 2019. In Sunlight, Vitamin D and Skin Cancer; Springer: Cham, Switzerland, 2020; pp. 123–139.
4. Fahradyan, A.; Howell, A.C.; Wolfswinkel, E.M.; Tsuha, M.; Sheth, P.; Wong, A.K. Updates on the management of non-melanoma skin cancer (NMSC). Healthcare 2017, 5, 82.
5. Ferlay, J.; Colombet, M.; Soerjomataram, I.; Mathers, C.; Parkin, D.M.; Piñeros, M.; Znaor, A.; Bray, F. Estimating the global cancer incidence and mortality in 2018: GLOBOCAN sources and methods. Int. J. Cancer 2019, 144, 1941–1953.

6. Khan, M.N.; Wang, Q.; Idrees, B.S.; Xiangli, W.; Teng, G.; Cui, X.; Zhao, Z.; Wei, K.; Abrar, M. A review on laser-induced breakdown spectroscopy in different cancers diagnosis and classification. Front. Phys. 2022, 10, 10.
7. Stevens, V.W.; Stenehjem, D.D.; Patterson, O.V.; Kamauu, A.W.; Yim, Y.M.; Morlock, R.J.; DuVall, S.L. Characterization and survival of patients with metastatic basal cell carcinoma in the Department of Veterans Affairs: A retrospective electronic health record review. Arch. Dermatol. Res. 2018, 310, 505–513.
8. Stiegel, E.; Lam, C.; Schowalter, M.; Somani, A.-K.; Lucas, J.; Poblete-Lopez, C. Correlation between original biopsy pathology and Mohs intraoperative pathology. Dermatol. Surg. 2018, 44, 193–197.
9. Khazaei, Z.; Ghorat, F.; Jarrahi, A.; Adineh, H.; Sohrabivafa, M.; Goodarzi, E. Global incidence and mortality of skin cancer by histological subtype and its relationship with the human development index (HDI)—An ecology study in 2018. World Cancer Res. J. 2019, 6, e13.
10. Ciążyńska, M.; Kamińska-Winciorek, G.; Lange, D.; Lewandowski, B.; Reich, A.; Sławińska, M.; Pabianek, M.; Szczepaniak, K.; Hankiewicz, A.; Ułańska, M. The incidence and clinical analysis of non-melanoma skin cancer. Sci. Rep. 2021, 11, 4337.
11. Popescu, D.; El-Khatib, M.; El-Khatib, H.; Ichim, L. New Trends in Melanoma Detection Using Neural Networks: A Systematic Review. Sensors 2022, 22, 496.
12. Ahlgrimm-Siess, V.; Laimer, M.; Arzberger, E.; Hofmann-Wellenhof, R. New diagnostics for melanoma detection: From artificial intelligence to RNA microarrays. Future Oncol. 2012, 8, 819–827.
13. Narayanan, D.L.; Saladi, R.N.; Fox, J.L. Ultraviolet radiation and skin cancer. Int. J. Dermatol. 2010, 49, 978–986.
14. Federico, M.B. SDG 3 Good Health and Well-Being. In Actioning the Global Goals for Local Impact; Springer: Berlin/Heidelberg, Germany, 2020; pp. 39–55.
15. Umar, S.A.; Tasduq, S.A. Ozone Layer Depletion and Emerging Public Health Concerns-An Update on Epidemiological Perspective of the Ambivalent Effects of Ultraviolet Radiation Exposure. Front. Oncol. 2022, 12, 866733.
16. Lin, T.-C.; Lee, H.-C. Skin cancer dermoscopy images classification with meta data via deep learning ensemble. In Proceedings of the 2020 International Computer Symposium (ICS), Tainan, Taiwan, 17–19 December 2020; pp. 237–241.
17. Kim, H.S.; Kim, H.J.; Hong, E.S.; Kim, K.B.; Lee, J.D.; Kang, T.U.; Ahn, H.S. The incidence and survival of melanoma and nonmelanoma skin cancer in patients with vitiligo: A nationwide population-based matched cohort study in Korea. Br. J. Dermatol. 2020, 182, 907–915.

18. Giaquinto, A.N.; Miller, K.D.; Tossas, K.Y.; Winn, R.A.; Jemal, A.; Siegel, R.L. Cancer statistics for African American/Black People 2022. CA A Cancer J. Clin. 2022, 72, 202–229.
19. Islami, F.; Guerra, C.E.; Minihan, A.; Yabroff, K.R.; Fedewa, S.A.; Sloan, K.; Wiedt, T.L.; Thomson, B.; Siegel, R.L.; Nargis, N. American Cancer Society's report on the status of cancer disparities in the United States, 2021. CA A Cancer J. Clin. 2022, 72, 112–143.
20. Iwagami, M.; Caplin, B.; Smeeth, L.; Tomlinson, L.A.; Nitsch, D. Clinical Codelist—Read Codes for Hypothyroidism; Data Collection; London School of Hygiene & Tropical Medicine: London, UK, 2018.
21. Arnold, M.; Singh, D.; Laversanne, M.; Vignat, J.; Vaccarella, S.; Meheus, F.; Cust, A.E.; de Vries, E.; Whiteman, D.C.; Bray, F. Global burden of cutaneous melanoma in 2020 and projections to 2040. JAMA Dermatol. 2022, 158, 495–503.
22. Di Carlo, V.; Stiller, C.A.; Eisemann, N.; Bordoni, A.; Matz, M.; Curado, M.P.; Daubisse-Marliac, L.; Valkov, M.; Bulliard, J.L.; Morrison, D. Does the morphology of cutaneous melanoma help explain the international differences in survival? Results from 1,578,482 adults diagnosed during 2000–2014 in 59 countries (CONCORD-3). Br. J. Dermatol. 2022, 187, 364–380.
23. Perez, E.; Ventura, S. Multi-view Deep Neural Networks for multiclass skin lesion diagnosis. In Proceedings of the 2022 IEEE International Conference on Omni-layer Intelligent Systems (COINS), Barcelona, Spain, 1–3 August 2022; pp. 1–6.
24. Siegel, R.; Ward, E.; Brawley, O.; Jemal, A. Cancer statistics, 2011: The impact of eliminating socioeconomic and racial disparities on premature cancer deaths. CA A Cancer J. Clin. 2011, 61, 212–236.
25. Gochi, A.; Orita, K.; Fuchimoto, S.; Tanaka, N.; Ogawa, N. The prognostic advantage of preoperative intratumoral injection of OK-432 for gastric cancer patients. Br. J. Cancer 2001, 84, 443–451.
26. Ishihara, K.; Saida, T.; Otsuka, F.; Yamazaki, N. Statistical profiles of malignant melanoma and other skin cancers in Japan: 2007 update. Int. J. Clin. Oncol. 2008, 13, 33–41.
27. Gloster, H.M., Jr.; Brodland, D.G. The epidemiology of skin cancer. Dermatol. Surg. 1996, 22, 217–226.
28. Reilly, P.; Cosh, J.; Maddison, P.; Rasker, J.; Silman, A. Mortality and survival in rheumatoid arthritis: A 25 year prospective study of 100 patients. Ann. Rheum. Dis. 1990, 49, 363–369.
29. Tseng, W.-P. Effects and dose-response relationships of skin cancer and blackfoot disease with arsenic. Environ. Health Perspect. 1977, 19, 109–119.
30. Phadke, J.G. Survival pattern and cause of death in patients with multiple sclerosis: Results from an epidemiological survey in north east Scotland. J. Neurol. Neurosurg. Psychiatry 1987, 50,

523–531.

31. Tsuchiya, K.; Aoyama, T.; Ju, M.; Atsumi, Y.; Kazama, K.; Numata, M.; Tamagawa, H.; Yukawa, N.; Rino, Y. A Case of Rectal Cancer with Brain and Skin Metastasis with Long-Term Survival Managed by Multidisciplinary Therapy. Gan Kagaku Ryoho 2022, 49, 1148–1150.
32. Celebi, M.E.; Iyatomi, H.; Schaefer, G.; Stoecker, W.V. Lesion border detection in dermoscopy images. Comput. Med. Imaging Graph. 2009, 33, 148–153.
33. Fernandes, S.L.; Chakraborty, B.; Gurupur, V.P.; Prabhu, G.A. Early skin cancer detection using computer aided diagnosis techniques. J. Integr. Des. Process. Sci. 2016, 20, 33–43.
34. Adla, D.; Reddy, G.; Nayak, P.; Karuna, G. Deep learning-based computer aided diagnosis model for skin cancer detection and classification. Distrib. Parallel Databases 2022, 40, 717–736.
35. Tsai, C.L.; Mukundan, A.; Chung, C.S.; Chen, Y.H.; Wang, Y.K.; Chen, T.H.; Tseng, Y.S.; Huang, C.W.; Wu, I.C.; Wang, H.C. Hyperspectral Imaging Combined with Artificial Intelligence in the Early Detection of Esophageal Cancer. Cancers 2021, 13, 4593.
36. Xu, Z.; Sheykhahmad, F.R.; Ghadimi, N.; Razmjooy, N. Computer-aided diagnosis of skin cancer based on soft computing techniques. Open Med. 2020, 15, 860–871.
37. Jaleel, J.A.; Salim, S.; Aswin, R. Computer aided detection of skin cancer. In Proceedings of the 2013 International Conference on Circuits, Power and Computing Technologies (ICCPCT), Nagercoil, India, 20–21 March 2013; pp. 1137–1142.
38. Kumar, K.A.; Vanmathi, C. Optimization driven model and segmentation network for skin cancer detection. Comput. Electr. Eng. 2022, 103, 108359.
39. Filali, Y.; EL Khoukhi, H.; Sabri, M.A.; Aarab, A. Efficient fusion of handcrafted and pre-trained CNNs features to classify melanoma skin cancer. Multimed. Tools Appl. 2020, 79, 31219–31238.
40. Mohanty, S.P.; Kougianos, E. Biosensors: A tutorial review. Ieee Potentials 2006, 25, 35–40.
41. Malibari, A.A.; Alzahrani, J.S.; Eltahir, M.M.; Malik, V.; Obayya, M.; Al Duhayyim, M.; Neto, A.V.L.; de Albuquerque, V.H.C. Optimal deep neural network-driven computer aided diagnosis model for skin cancer. Comput. Electr. Eng. 2022, 103, 108318.
42. Bratchenko, I.A.; Bratchenko, L.A.; Moryatov, A.A.; Khristoforova, Y.A.; Artemyev, D.N.; Myakinin, O.O.; Orlov, A.E.; Kozlov, S.V.; Zakharov, V.P. In vivo diagnosis of skin cancer with a portable Raman spectroscopic device. Exp. Dermatol. 2021, 30, 652–663.
43. Bohunicky, B.; Mousa, S. Biosensors: The new wave in cancer diagnosis. Nanotechnol. Sci. Appl. 2010, 4, 1–10.
44. Keshavarz, A.; Vafapour, Z. Water-based terahertz metamaterial for skin cancer detection application. IEEE Sens. J. 2018, 19, 1519–1524.

45. Lalitha, K.; Lakshmi, K. An overview on biosensors. Int. J. Pharm. Chem. Biol. Sci. 2017, 7, 293–302.
46. Ashraf, R.; Afzal, S.; Rehman, A.U.; Gul, S.; Baber, J.; Bakhtyar, M.; Mehmood, I.; Song, O.-Y.; Maqsood, M. Region-of-interest based transfer learning assisted framework for skin cancer detection. IEEE Access 2020, 8, 147858–147871.
47. Alheejawi, S.; Xu, H.; Berendt, R.; Jha, N.; Mandal, M. Novel lymph node segmentation and proliferation index measurement for skin melanoma biopsy images. Comput. Med. Imaging Graph. 2019, 73, 19–29.
48. Vocaturo, E.; Perna, D.; Zumpano, E. Machine learning techniques for automated melanoma detection. In Proceedings of the 2019 IEEE International Conference on Bioinformatics and Biomedicine (BIBM), San Diego, CA, USA, 18–21 November 2019; pp. 2310–2317.
49. Rey-Barroso, L.; Peña-Gutiérrez, S.; Yáñez, C.; Burgos-Fernández, F.J.; Vilaseca, M.; Royo, S. Optical technologies for the improvement of skin cancer diagnosis: A review. Sensors 2021, 21, 252.
50. Jiang, S.; Li, H.; Jin, Z. A visually interpretable deep learning framework for histopathological image-based skin cancer diagnosis. IEEE J. Biomed. Health Inform. 2021, 25, 1483–1494.
51. Saba, T. Computer vision for microscopic skin cancer diagnosis using handcrafted and non-handcrafted features. Microsc. Res. Tech. 2021, 84, 1272–1283.
52. Kumar, M.; Alshehri, M.; AlGhamdi, R.; Sharma, P.; Deep, V. A de-ann inspired skin cancer detection approach using fuzzy c-means clustering. Mob. Netw. Appl. 2020, 25, 1319–1329.
53. Premaladha, J.; Ravichandran, K. Novel approaches for diagnosing melanoma skin lesions through supervised and deep learning algorithms. J. Med. Syst. 2016, 40, 96.
54. Afifi, S.; GholamHosseini, H.; Sinha, R. SVM classifier on chip for melanoma detection. Annu. Int. Conf. IEEE Eng. Med. Biol. Soc. 2017, 2017, 270–274.
55. Thiem, D.G.; Römer, P.; Blatt, S.; Al-Nawas, B.; Kämmerer, P.W. New Approach to the Old Challenge of Free Flap Monitoring—Hyperspectral Imaging Outperforms Clinical Assessment by Earlier Detection of Perfusion Failure. J. Pers. Med. 2021, 11, 1101.
56. Ghamisi, P.; Rasti, B.; Yokoya, N.; Wang, Q.; Hofle, B.; Bruzzone, L.; Bovolo, F.; Chi, M.; Anders, K.; Gloaguen, R. Multisource and multitemporal data fusion in remote sensing: A comprehensive review of the state of the art. IEEE Geosci. Remote Sens. Mag. 2019, 7, 6–39.
57. Li, Q.; He, X.; Wang, Y.; Liu, H.; Xu, D.; Guo, F. Review of spectral imaging technology in biomedical engineering: Achievements and challenges. J. Biomed. Opt. 2013, 18, 100901.
58. Lu, G.; Fei, B. Medical hyperspectral imaging: A review. J. Biomed. Opt. 2014, 19, 010901.

59. Zakian, C.M.; Pretty, I.A.; Ellwood, R. Near-infared hyperspectral imaging of teeth for dental caries detection. J. Biomed. Opt. 2009, 14, 064047.
60. Tromberg, B.J.; Shah, N.; Lanning, R.; Cerussi, A.; Espinoza, J.; Pham, T.; Svaasand, L.; Butler, J. Non-invasive in vivo characterization of breast tumors using photon migration spectroscopy. Neoplasia 2000, 2, 26–40.
61. Cerussi, A.E.; Berger, A.J.; Bevilacqua, F.; Shah, N.; Jakubowski, D.; Butler, J.; Holcombe, R.F.; Tromberg, B.J. Sources of absorption and scattering contrast for near-infrared optical mammography. Acad. Radiol. 2001, 8, 211–218.
62. Bi, D.; Zhu, D.; Sheykhahmad, F.R.; Qiao, M. Computer-aided skin cancer diagnosis based on a New meta-heuristic algorithm combined with support vector method. Biomed. Signal Process. Control 2021, 68, 102631.
63. Barducci, A.; Guzzi, D.; Marcoionni, P.; Pippi, I. Aerospace wetland monitoring by hyperspectral imaging sensors: A case study in the coastal zone of San Rossore Natural Park. J. Environ. Manag. 2009, 90, 2278–2286.
64. Sun, D.-W. Hyperspectral Imaging for Food Quality Analysis and Control; Elsevier: Amsterdam, The Netherlands, 2010.
65. Lu, B.; Dao, P.D.; Liu, J.; He, Y.; Shang, J. Recent advances of hyperspectral imaging technology and applications in agriculture. Remote Sens. 2020, 12, 2659.
66. Fei, B. Hyperspectral imaging in medical applications. In Data Handling in Science and Technology; Elsevier: Amsterdam, The Netherlands, 2020; Volume 32, pp. 523–565.
67. Lee, C.-H.; Mukundan, A.; Chang, S.-C.; Wang, Y.-L.; Lu, S.-H.; Huang, Y.-C.; Wang, H.-C. Comparative Analysis of Stress and Deformation between One-Fenced and Three-Fenced Dental Implants Using Finite Element Analysis. J. Clin. Med. 2021, 10, 3986.
68. Hege, E.K.; O'Connell, D.; Johnson, W.; Basty, S.; Dereniak, E.L. Hyperspectral imaging for astronomy and space surveillance. Imaging Spectrom. IX 2004, 5159, 380–391.
69. Courtenay, L.A.; González-Aguilera, D.; Lagüela, S.; Del Pozo, S.; Ruiz-Mendez, C.; Barbero-García, I.; Román-Curto, C.; Cañueto, J.; Santos-Durán, C.; Cardeñoso-Álvarez, M.E. Hyperspectral imaging and robust statistics in non-melanoma skin cancer analysis. Biomed. Opt. Express 2021, 12, 5107–5127.
70. Tsai, T.-J.; Mukundan, A.; Chi, Y.-S.; Tsao, Y.-M.; Wang, Y.-K.; Chen, T.-H.; Wu, I.-C.; Huang, C.-W.; Wang, H.-C. Intelligent Identification of Early Esophageal Cancer by Band-Selective Hyperspectral Imaging. Cancers 2022, 14, 4292.
71. Fang, Y.-J.; Mukundan, A.; Tsao, Y.-M.; Huang, C.-W.; Wang, H.-C. Identification of Early Esophageal Cancer by Semantic Segmentation. J. Pers. Med. 2022, 12, 1204.

72. Aboughaleb, I.H.; Aref, M.H.; El-Sharkawy, Y.H. Hyperspectral imaging for diagnosis and detection of ex-vivo breast cancer. Photodiagnosis Photodyn. Ther. 2020, 31, 101922.
73. Liu, H.; Yu, T.; Hu, B.; Hou, X.; Zhang, Z.; Liu, X.; Liu, J.; Wang, X.; Zhong, J.; Tan, Z. Uav-borne hyperspectral imaging remote sensing system based on acousto-optic tunable filter for water quality monitoring. Remote Sens. 2021, 13, 4069.
74. Liu, H.; Bruning, B.; Garnett, T.; Berger, B. Hyperspectral imaging and 3D technologies for plant phenotyping: From satellite to close-range sensing. Comput. Electron. Agric. 2020, 175, 105621.
75. Shrestha, S.; Knapič, M.; Žibrat, U.; Deleuran, L.C.; Gislum, R. Single seed near-infrared hyperspectral imaging in determining tomato (Solanum lycopersicum L.) seed quality in association with multivariate data analysis. Sens. Actuators B Chem. 2016, 237, 1027–1034.
76. Wu, N.; Liu, F.; Meng, F.; Li, M.; Zhang, C.; He, Y. Rapid and accurate varieties classification of different crop seeds under sample-limited condition based on hyperspectral imaging and deep transfer learning. Front. Bioeng. Biotechnol. 2021, 9, 696292.
77. Hsiao, Y.-P.; Mukundan, A.; Chen, W.-C.; Wu, M.-T.; Hsieh, S.-C.; Wang, H.-C. Design of a Lab-On-Chip for Cancer Cell Detection through Impedance and Photoelectrochemical Response Analysis. Biosensors 2022, 12, 405.
78. Stuart, M.B.; McGonigle, A.J.; Willmott, J.R. Hyperspectral imaging in environmental monitoring: A review of recent developments and technological advances in compact field deployable systems. Sensors 2019, 19, 3071.
79. Chen, C.-W.; Tseng, Y.-S.; Mukundan, A.; Wang, H.-C. Air Pollution: Sensitive Detection of PM2.5 and PM10 Concentration Using Hyperspectral Imaging. Appl. Sci. 2021, 11, 4543.
80. Huang, S.-Y.; Mukundan, A.; Tsao, Y.-M.; Kim, Y.; Lin, F.-C.; Wang, H.-C. Recent Advances in Counterfeit Art, Document, Photo, Hologram, and Currency Detection Using Hyperspectral Imaging. Sensors 2022, 22, 7308.
81. Mukundan, A.; Tsao, Y.-M.; Lin, F.-C.; Wang, H.-C. Portable and low-cost hologram verification module using a snapshot-based hyperspectral imaging algorithm. Sci. Rep. 2022, 12, 18475.
82. Mukundan, A.; Wang, H.-C.; Tsao, Y.-M. A Novel Multipurpose Snapshot Hyperspectral Imager used to Verify Security Hologram. In Proceedings of the 2022 International Conference on Engineering and Emerging Technologies (ICEET), Kuala Lumpur, Malaysia, 27–28 October 2022; pp. 1–3.
83. Mukundan, A.; Tsao, Y.-M.; Cheng, W.-M.; Lin, F.-C.; Wang, H.-C. Automatic Counterfeit Currency Detection Using a Novel Snapshot Hyperspectral Imaging Algorithm. Sensors 2023, 23, 2026.
84. Hamilton, S.J.; Lodder, R.A. Hyperspectral imaging technology for pharmaceutical analysis. Biomed. Nanotechnol. Archit. Appl. 2002, 4626, 136–147.

85. Chang, L.; Zhang, M.; Li, W. A coarse-to-fine approach for medical hyperspectral image classification with sparse representation. AOPC 2017 Opt. Spectrosc. Imaging 2017, 10461, 136–144.

86. Yang, K.-Y.; Fang, Y.-J.; Karmakar, R.; Mukundan, A.; Tsao, Y.-M.; Huang, C.-W.; Wang, H.-C. Assessment of Narrow Band Imaging Algorithm for Video Capsule Endoscopy Based on Decorrelated Color Space for Esophageal Cancer. Cancers 2023, 15, 4715.

87. de la Ossa, M.Á.F.; Amigo, J.M.; García-Ruiz, C. Detection of residues from explosive manipulation by near infrared hyperspectral imaging: A promising forensic tool. Forensic Sci. Int. 2014, 242, 228–235.

88. Favreau, P.F.; Hernandez, C.; Lindsey, A.S.; Alvarez, D.F.; Rich, T.C.; Prabhat, P.; Leavesley, S.J. Thin-film tunable filters for hyperspectral fluorescence microscopy. J. Biomed. Opt. 2013, 19, 011017.

89. Xu, D.; Ni, G.; Jiang, T.; Jiang, L.; Chi, M. Integration of field work and hyperspectral data for oil and gas exploration. In Proceedings of the 2007 IEEE International Geoscience and Remote Sensing Symposium, Barcelona, Spain, 23–28 July 2007; pp. 3194–3197.

90. Gowen, A.A.; Feng, Y.; Gaston, E.; Valdramidis, V. Recent applications of hyperspectral imaging in microbiology. Talanta 2015, 137, 43–54.

91. Wang, Y.; Hu, X.; Hou, Z.; Ning, J.; Zhang, Z. Discrimination of nitrogen fertilizer levels of tea plant (Camellia sinensis) based on hyperspectral imaging. J. Sci. Food Agric. 2018, 98, 4659–4664.

92. Huang, S.; Wang, L.; Chen, W.; Lin, D.; Huang, L.; Wu, S.; Feng, S.; Chen, R. Non-invasive optical detection of esophagus cancer based on urine surface-enhanced Raman spectroscopy. In Proceedings of the Twelfth International Conference on Photonics and Imaging in Biology and Medicine (PIBM 2014), Wuhan, China, 17 September 2014; pp. 537–542.

93. Zabalza, J.; Ren, J.; Wang, Z.; Marshall, S.; Wang, J. Singular spectrum analysis for effective feature extraction in hyperspectral imaging. IEEE Geosci. Remote Sens. Lett. 2014, 11, 1886–1890.

94. Fabelo, H.; Ortega, S.; Lazcano, R.; Madroñal, D.; Callicó, G.M.; Juárez, E.; Salvador, R.; Bulters, D.; Bulstrode, H.; Szolna, A. An intraoperative visualization system using hyperspectral imaging to aid in brain tumor delineation. Sensors 2018, 18, 430.

95. More, S.S.; Beach, J.M.; McClelland, C.; Mokhtarzadeh, A.; Vince, R. In vivo assessment of retinal biomarkers by hyperspectral imaging: Early detection of Alzheimer’s disease. ACS Chem. Neurosci. 2019, 10, 4492–4501.

96. Chang, C.-I.; Wu, C.-C.; Liu, K.-H.; Chen, H.-M.; Chen, C.C.-C.; Wen, C.-H. Progressive band processing of linear spectral unmixing for hyperspectral imagery. IEEE J. Sel. Top. Appl. Earth Obs. Remote Sens. 2014, 8, 2583–2597.

97. Akbari, H.; Halig, L.V.; Zhang, H.; Wang, D.; Chen, Z.G.; Fei, B. Detection of cancer metastasis using a novel macroscopic hyperspectral method. In Proceedings of the Medical Imaging 2012: Biomedical Applications in Molecular, Structural, and Functional Imaging, San Diego, CA, USA, 14 April 2012; pp. 299–305.
98. Senan, E.M.; Jadhav, M.E. Classification of dermoscopy images for early detection of skin cancer —A review. Int. J. Comput. Appl. 2019, 975, 8887.
99. Esteva, A.; Kuprel, B.; Novoa, R.A.; Ko, J.; Swetter, S.M.; Blau, H.M.; Thrun, S. Dermatologist-level classification of skin cancer with deep neural networks. Nature 2017, 542, 115–118.
100. Ortega, S.; Fabelo, H.; Iakovidis, D.K.; Koulaouzidis, A.; Callico, G.M. Use of hyperspectral/multispectral imaging in gastroenterology. Shedding some–different–light into the dark. J. Clin. Med. 2019, 8, 36.
101. Nachbar, F.; Stolz, W.; Merkle, T.; Cognetta, A.B.; Vogt, T.; Landthaler, M.; Bilek, P.; Braun-Falco, O.; Plewig, G. The ABCD rule of dermatoscopy: High prospective value in the diagnosis of doubtful melanocytic skin lesions. J. Am. Acad. Dermatol. 1994, 30, 551–559.
102. Tsao, H.; Olazagasti, J.M.; Cordoro, K.M.; Brewer, J.D.; Taylor, S.C.; Bordeaux, J.S.; Chren, M.-M.; Sober, A.J.; Tegeler, C.; Bhushan, R. Early detection of melanoma: Reviewing the ABCDEs. J. Am. Acad. Dermatol. 2015, 72, 717–723.
103. Peters, M.S.; Winkelmann, R.K. The biopsy. Dermatol. Clin. 1984, 2, 209–217.
104. Wollina, U.; Burroni, M.; Torricelli, R.; Gilardi, S.; Dell'Eva, G.; Helm, C.; Bardey, W. Digital dermoscopy in clinical practise: A three-centre analysis. Ski. Res. Technol. 2007, 13, 133–142.
105. Tudor, A.; Feldman, J.; Diamandis, C. Why the ABCDE Rule Is Not Helpful but Dangerous in Skin Cancer Prevention. Zenodo, 27 November 2021. Available online: https://www.scanoma.com/blog/why-the-abcde-rule-is-not-helpful-but-dangerous-in-skin-cancer-prevention (accessed on 26 November 2023).
106. Fabelo, H.; Melián, V.; Martínez, B.; Beltrán, P.; Ortega, S.; Marrero, M.; Callicó, G.M.; Sarmiento, R.; Castaño, I.; Carretero, G. Dermatologic hyperspectral imaging system for skin cancer diagnosis assistance. In Proceedings of the 2019 XXXIV Conference on Design of Circuits and Integrated Systems (DCIS), Bilbao, Spain, 20–22 November 2019; pp. 1–6.
107. Jain, S.; Pise, N. Computer aided melanoma skin cancer detection using image processing. Procedia Comput. Sci. 2015, 48, 735–740.
108. Serao, N.; Delfino, K.; Southey, B.; Zas, S.R. Development of a transcriptomic-based index to prognosticate cancer. ISBRA 2010 2010, 2010, 42.
109. Carli, P.; Quercioli, E.; Sestini, S.; Stante, M.; Ricci, L.; Brunasso, G.; De Giorgi, V. Pattern analysis, not simplified algorithms, is the most reliable method for teaching dermoscopy for

melanoma diagnosis to residents in dermatology. Br. J. Dermatol. 2003, 148, 981–984.

110. Kasmi, R.; Mokrani, K. Classification of malignant melanoma and benign skin lesions: Implementation of automatic ABCD rule. IET Image Process. 2016, 10, 448–455.
111. Ali, A.-R.H.; Li, J.; Yang, G. Automating the ABCD rule for melanoma detection: A survey. IEEE Access 2020, 8, 83333–83346.
112. Ahnlide, I.; Bjellerup, M.; Nilsson, F.; Nielsen, K. Validity of ABCD rule of dermoscopy in clinical practice. Acta Derm. Venereol. 2016, 96, 367–372.
113. Binder, M.; Kittler, H.; Steiner, A.; Dawid, M.; Pehamberger, H.; Wolff, K. Reevaluation of the ABCD rule for epiluminescence microscopy. J. Am. Acad. Dermatol. 1999, 40, 171–176.
114. Milton, M.A.A. Automated skin lesion classification using ensemble of deep neural networks in ISIC 2018: Skin lesion analysis towards melanoma detection challenge. arXiv 2019, arXiv:1901.10802.
115. Basov, S.; Dankner, Y.; Weinstein, M.; Katzir, A.; Platkov, M. Noninvasive mid-IR fiber-optic evanescent wave spectroscopy (FEWS) for early detection of skin cancers. Med. Phys. 2020, 47, 5523–5530.
116. Saba, T. Recent advancement in cancer detection using machine learning: Systematic survey of decades, comparisons and challenges. J. Infect. Public Health 2020, 13, 1274–1289.
117. Jerant, A.F.; Johnson, J.T.; Sheridan, C.D.; Caffrey, T.J. Early detection and treatment of skin cancer. Am. Fam. Physician 2000, 62, 357–368.
118. Ragab, M.; Choudhry, H.; Al-Rabia, M.W.; Binyamin, S.S.; Aldarmahi, A.A.; Mansour, R.F. Early and accurate detection of melanoma skin cancer using hybrid level set approach. Front. Physiol. 2022, 13, 965630.
119. Masood, A.; Ali Al-Jumaily, A. Computer aided diagnostic support system for skin cancer: A review of techniques and algorithms. Int. J. Biomed. Imaging 2013, 2013, 323268.
120. Johr, R.H. Dermoscopy: Alternative melanocytic algorithms—The ABCD rule of dermatoscopy, menzies scoring method, and 7-point checklist. Clin. Dermatol. 2002, 20, 240–247.
121. Kumar, Y.; Gupta, S.; Singla, R.; Hu, Y.-C. A systematic review of artificial intelligence techniques in cancer prediction and diagnosis. Arch. Comput. Methods Eng. 2021, 29, 2043–2070.
122. Abbasi, N.R.; Shaw, H.M.; Rigel, D.S.; Friedman, R.J.; McCarthy, W.H.; Osman, I.; Kopf, A.W.; Polsky, D. Early diagnosis of cutaneous melanoma: Revisiting the ABCD criteria. JAMA 2004, 292, 2771–2776.
123. Burlina, P.; Billings, S.; Joshi, N.; Albayda, J. Automated diagnosis of myositis from muscle ultrasound: Exploring the use of machine learning and deep learning methods. PLoS ONE 2017,

12, e0184059.

124. Chilamkurthy, S.; Ghosh, R.; Tanamala, S.; Biviji, M.; Campeau, N.G.; Venugopal, V.K.; Mahajan, V.; Rao, P.; Warier, P. Deep learning algorithms for detection of critical findings in head CT scans: A retrospective study. Lancet 2018, 392, 2388–2396.
125. Bianconi, F.; Fravolini, M.L.; Pizzoli, S.; Palumbo, I.; Minestrini, M.; Rondini, M.; Nuvoli, S.; Spanu, A.; Palumbo, B. Comparative evaluation of conventional and deep learning methods for semi-automated segmentation of pulmonary nodules on CT. Quant. Imaging Med. Surg. 2021, 11, 3286.
126. Javed, R.; Rahim, M.S.M.; Saba, T.; Rehman, A. A comparative study of features selection for skin lesion detection from dermoscopic images. Netw. Model. Anal. Health Inform. Bioinform. 2020, 9, 4.
127. Hagerty, J.R.; Stanley, R.J.; Almubarak, H.A.; Lama, N.; Kasmi, R.; Guo, P.; Drugge, R.J.; Rabinovitz, H.S.; Oliviero, M.; Stoecker, W.V. Deep learning and handcrafted method fusion: Higher diagnostic accuracy for melanoma dermoscopy images. IEEE J. Biomed. Health Inform. 2019, 23, 1385–1391.
128. Zhu, W.; Zeng, N.; Wang, N. Sensitivity, specificity, accuracy, associated confidence interval and ROC analysis with practical SAS implementations. NESUG Proc. Health Care Life Sci. Baltim. Md. 2010, 19, 67.
129. Matinfar, M.; Shahidi, S.; Feizi, A. Incidence of nonmelanoma skin cancer in renal transplant recipients: A systematic review and meta-analysis. J. Res. Med. Sci. Off. J. Isfahan Univ. Med. Sci. 2018, 23, 14.
130. Gandini, S.; Palli, D.; Spadola, G.; Bendinelli, B.; Cocorocchio, E.; Stanganelli, I.; Miligi, L.; Masala, G.; Caini, S. Anti-hypertensive drugs and skin cancer risk: A review of the literature and meta-analysis. Crit. Rev. Oncol. Hematol. 2018, 122, 1–9.
131. Sharon, E.; Snast, I.; Lapidoth, M.; Kaftory, R.; Mimouni, D.; Hodak, E.; Levi, A. Laser treatment for non-melanoma skin cancer: A systematic review and meta-analysis. Am. J. Clin. Dermatol. 2021, 22, 25–38.
132. Arafa, A.; Mostafa, A.; Navarini, A.A.; Dong, J.-Y. The association between smoking and risk of skin cancer: A meta-analysis of cohort studies. Cancer Causes Control 2020, 31, 787–794.
133. Jiyad, Z.; Olsen, C.; Burke, M.; Isbel, N.; Green, A.C. Azathioprine and risk of skin cancer in organ transplant recipients: Systematic review and meta-analysis. Am. J. Transplant. 2016, 16, 3490–3503.
134. Glas, A.S.; Lijmer, J.G.; Prins, M.H.; Bonsel, G.J.; Bossuyt, P.M. The diagnostic odds ratio: A single indicator of test performance. J. Clin. Epidemiol. 2003, 56, 1129–1135.

135. Duke, A.A.; Bègue, L.; Bell, R.; Eisenlohr-Moul, T. Revisiting the serotonin–aggression relation in humans: A meta-analysis. Psychol. Bull. 2013, 139, 1148.

136. Song, J.; Wan, S.; Piao, S.; Knapp, A.K.; Classen, A.T.; Vicca, S.; Ciais, P.; Hovenden, M.J.; Leuzinger, S.; Beier, C. A meta-analysis of 1119 manipulative experiments on terrestrial carbon-cycling responses to global change. Nat. Ecol. Evol. 2019, 3, 1309–1320.

137. Cartiff, B.M.; Duke, R.F.; Greene, J.A. The effect of epistemic cognition interventions on academic achievement: A meta-analysis. J. Educ. Psychol. 2021, 113, 477.

138. Greene, J.A.; Cartiff, B.M.; Duke, R.F. A meta-analytic review of the relationship between epistemic cognition and academic achievement. J. Educ. Psychol. 2018, 110, 1084.